

# Interfacial defects of hard magnetic $\text{Pr}_2\text{Fe}_{14}\text{B}$ phase from amorphous to nanostructures<sup>①</sup>

WU Yur-cheng(吴玉程)

(Faculty of Materials Science and Engineering, Hefei University of Technology, Hefei 230009, China)

**Abstract:** The interfacial defects of hard magnetic  $\text{Pr}_2\text{Fe}_{14}\text{B}$  phase from amorphous to nanostructures have been investigated by positron lifetime spectroscopy. The nanostructure was produced by melt-spinning and nanocrystallization route. The two main components can be ascribed to vacancy-like defects in the intergranular layers or the interfaces, and microvoids or large free volumes with size compared to several missing atoms at the interactions of the atomic aggregates or the crystallites. The remarkable changes in the positron lifetimes from the amorphous structure to the nanostructure with varied sizes can be interpreted, indicating that the structural transformation and the grain growth induce the defect changes occurring at the interfaces with different shapes and sizes.

**Key words:**  $\text{Pr}_2\text{Fe}_{14}\text{B}$ ; amorphous; nanostructure; interfacial structure

**CLC number:** TB 383; TM 271

**Document code:** A

## 1 INTRODUCTION

Despite the great technical relevance of  $(\text{Nd}, \text{Pr})_2\text{Fe}_{14}\text{B}$  as high-performance permanent magnet, and extensive studies have been devoted to magnetic performance and microstructure, no concrete data on the microstructural features such as interfacial structure of the grain boundary and defects distribution, as well as the self-diffusion in this system have been obtained.  $(\text{Nd}, \text{Pr})_2\text{Fe}_{14}\text{B}$  single hard phase is chosen to study the microstructure and diffusion in order to prevent the effect of the rare-earth metal-rich phase emerged in the grain boundary of the hyperstoichiometrically compositional magnet<sup>[1,2]</sup>.  $\text{Pr}_2\text{Fe}_{14}\text{B}$  is preferentially used to investigate the details in microstructure and diffusion because of the magnetic advantages although it owns the isostructure of  $\text{Nd}_2\text{Fe}_{14}\text{B}$ . In addition, the metallurgical processes of these materials involve sintering and hot pressing accompanied with creep, corrosion, solid-state transformations and penetration of impurities, which are related to the diffusion and the characteristics of the interfacial structures<sup>[3,4]</sup>. An understanding of these properties requires a detailed study of the atomic structure of the interfaces, particularly of their structural free volumes, and of the atomic transport behavior at the interfaces.

Positron annihilation is an ideal tool to investigate the microstructure of materials, which can be particularly used for the study of the interfacial struc-

ture of nanocrystalline solids<sup>[5]</sup>. Some information about free volumes on an atomic scale, e. g., vacancy-like defects in disordered media is available with positron lifetime spectroscopy, because it yields a measure for the size of these free volumes. In this paper, the free volume distributions have been investigated at room temperature using positron lifetime spectroscopy on amorphous and nanocrystalline  $\text{Pr}_2\text{Fe}_{14}\text{B}$  samples, produced by melt-spinning and nanocrystallization route.

## 2 EXPERIMENTAL

The studied amorphous  $\text{Pr}_2\text{Fe}_{14}\text{B}$  ribbons containing 3.0% (mole fraction) Zr, had a size of 25  $\mu\text{m}$  in thickness and 4 - 5 mm in width and were produced by melt-spinning method. Using the nanocrystallization route from the amorphous structure ribbon under different annealing conditions hence created the nanocrystalline alloy specimens with a variation of grain sizes. The amorphous ribbons were firstly heated in high vacuum atmosphere  $2.0 \times 10^{-8}$  Pa at relatively lower temperatures ranging from 200  $^\circ\text{C}$  to 570  $^\circ\text{C}$ , the changes of the positron lifetime in the relaxed amorphous  $\text{Pr}_2\text{Fe}_{14}\text{B}$  were expected during the structural relaxation. Then, after the nanocrystallization of the amorphous specimen at 680  $^\circ\text{C}$  for 2 min, the resultant nanocrystalline  $\text{Pr}_2\text{Fe}_{14}\text{B}$  was isothermally heated at 680  $^\circ\text{C}$ , leading to a variation of the grain growth with the annealing time, so the free volume

① **Foundation item:** Project(Wu 191/4-1) supported by the Land Baden Württemberg and Max-Planck-Institut für Metallforschung, Germany, as well as the Deutsche Forschungsgemeinschaft; Project(030304B2) sponsored by the Scientific Research Foundation for the Returned Overseas Chinese Scholars, State Education Ministry, China

**Received date:** 2003-10-10; **Accepted date:** 2004-03-18

**Correspondence:** Wu Yur-cheng, Professor, PhD; Tel: + 86-551-2901362; E-mail: ycwu@issp.ac.cn

variation with the change of the grain size could be studied.

X-ray diffraction (XRD) was performed using a Siemens D500 diffractometer with  $\text{CuK}\alpha$  radiation, and a graphite monochromator, operating at 30 mA, 40 kV. The  $\text{Pr}_2\text{Fe}_{14}\text{B}$  ribbons for the positron lifetime spectrum measurements were prepared by stacking 15–20 several-layer thick sheets to ensure that the positron from  $^{22}\text{Na}$  source annihilated within the material only. The  $^{22}\text{Na}$  positron source with activity  $1.3 \times 10^6$  Bq packed on a 0.8  $\mu\text{m}$  thick Al foil was sandwiched between the two parts of the specimen. The time resolution, or full width at half-maximum (FWHM), was around 210–220 ps using a  $\text{BaF}_2$  scintillator counter and the channel width 12.3 ps. More than  $10^7$  counts were recorded in each measurement, and the data analysis was performed using the posfit computer program.

### 3 RESULTS AND DISCUSSION

The crystallization process of the amorphous structure and the grain growth of the resultant nanocrystalline structures were evidenced by XRD, as shown in Fig. 1. The typical broad maximum corresponding to the amorphous structure can be seen around  $2\theta \approx 45^\circ$  in the specimen. It is obvious that the material annealed at 400  $^\circ\text{C}$  for 120 min was still in the amorphous state, and no crystallizing nucleation could be detected by the experiment. After annealing at 475  $^\circ\text{C}$  up to a higher temperature, a little degree of crystallization in the specimens can be ascertained from XRD. Therefore, the amorphous ribbons can be prepared for a representative set of relaxed amorphous structure samples characterized by different microstructure states, in which we can check the changes of the distributions of the free volumes from the positron lifetimes.

The dependence of the crystallization evolution on the annealing time can be clearly seen in the XRD patterns, exhibiting that the microstructure of nanocrystalline  $\text{Pr}_2\text{Fe}_{14}\text{B}$  varied with increasing grain size when subjected to annealing at 680  $^\circ\text{C}$  with changing time. The amorphous  $\text{Pr}_2\text{Fe}_{14}\text{B}$  crystallized after heating at 680  $^\circ\text{C}$  for 2 min, but the diffraction was still in wide distribution. This shows an imperfect crystallization of the amorphous precursor, or that the resultant nanocrystalline has still quite small grain sizes in the initial crystallizing state. Increasing the annealing time, the diffraction peaks became sharper indicating the further crystallization and grain growth. When the annealing time exceeded 180 min at 680  $^\circ\text{C}$ , the nanocrystalline  $\text{Pr}_2\text{Fe}_{14}\text{B}$  remarkably gave rise to some diffraction changes with high intensity that can be ascribed to grain growth with larger sizes. The grain size distribution measurements were

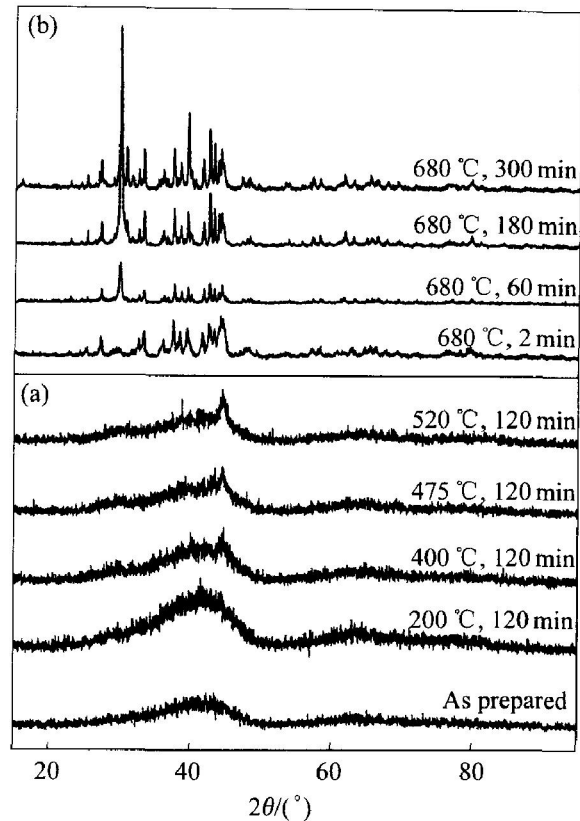


**Fig. 1** XRD patterns of amorphous and nanocrystalline  $\text{Pr}_2\text{Fe}_{14}\text{B}$

- (a) —As prepared amorphous phase isochronally heated for 120 min from 200  $^\circ\text{C}$  to 520  $^\circ\text{C}$ ;  
 (b) —Nanocrystalline obtained by nanocrystallization at 680  $^\circ\text{C}$  for 2 min isothermally annealed from 5 to 300 min

performed from the X-ray diffraction peak broadening. The grain size increased with the annealing time up to 300 min but within 100 nm due to the addition of 3.0% (mole fraction) Zr in  $\text{Pr}_2\text{Fe}_{14}\text{B}$ .

The trapping of a positron results in a prolonged lifetime compared to the positron lifetime for perfect crystallites<sup>[6]</sup>. The positron lifetime spectroscopy for the as prepared amorphous phase and the initial nanocrystalline  $\text{Pr}_2\text{Fe}_{14}\text{B}$  are shown in Fig. 2. It can be found that two dominant positron lifetime components, a short lifetime,  $\tau_1$ , and an intermediate lifetime  $\tau_2$ , as well as a weak third long-life component,  $\tau_3 > 1000$  ps (the third long-lived component of faint 1%–2% intensity was subtracted from the spectra in the final analysis), can be discerned. The as-prepared amorphous specimen has a lifetime of 208 ps ( $\tau_1$ ) with an intensity of nearly 90%. Similarly, the nanocrystalline characterized first component having lifetime 181 ps with intensity 95%, indicates that they have the same defect distribution characteristic from the amorphous to the initial nanocrystalline structure. Dittmar et al<sup>[7]</sup> convinced that in nanocrystalline  $\text{Fe}_{73.5}\text{Si}_{13.5}\text{B}_9\text{Nb}_3\text{Cu}_1$  a single lifetime  $\tau_1 = 144$  ps identical to that in the amorphous state was observed at ambient temperature, which characterizes free volumes with a reduced size compared to a lattice

vacancy. This was considered to be attributed to positron trapping and annihilation in amorphous intergranular layers.

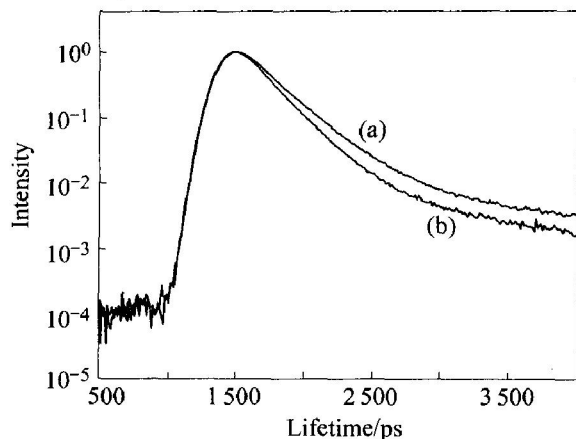


**Fig. 2** Positron lifetime spectra of as-prepared amorphous (a) and nanocrystalline (b)  $\text{Pr}_2\text{Fe}_{14}\text{B}$  prepared at  $680\text{ }^\circ\text{C}$  for 2 min

According to the correlations between electron density and free positron lifetime<sup>[8]</sup>, we can estimate the positron lifetimes of the  $\text{Pr}_2\text{Fe}_{14}\text{B}$  to 115–120 ps for a defect-free crystallite and 175 ps for a single vacancy, respectively. Interfaces of different size and shape probably appear more or less identical to positrons, which, after trapping, probe the local disorder at an atomic scale. Thus, we can confirm that the first component is attributed to intergranular free volumes compared to one vacancy and the second to larger voids for the amorphous  $\text{Pr}_2\text{Fe}_{14}\text{B}$ .

Nagel et al<sup>[9]</sup> reported that one single lifetime in metallic glasses is generally observed and interpreted in terms of complete trapping of positrons into the high number of cavities of different size on the atomic scale, indicating irregular arrays of potential wells with different binding strength. The studied amorphous  $\text{Pr}_2\text{Fe}_{14}\text{B}$  also nearly has one component with prevailing intensity, but the difference shows obviously that the free volumes are remarkably larger in size equally to several vacancies. However, the nanocrystalline  $\text{Pr}_2\text{Fe}_{14}\text{B}$  showed two main components corresponding to vacancy-sized free volumes in the interfaces and to microvoids located among the crystallites. But the first component of the initial nanocrystalline  $\text{Pr}_2\text{Fe}_{14}\text{B}$  also had a great intensity like in the amorphous structure. The problem is that the nanocrystalline seems actually in the starting crystallization stage from the amorphous state, i. e., the grain size is about 20 nm. This gave us a message that the nanocrystalline  $\text{Pr}_2\text{Fe}_{14}\text{B}$  inherited the structural features of the amorphous structure, especially in the interfaces, because it owns a small grain size and a large number of interfaces. Many results also suggested that, for nanocrystallization route the crystallization usually can not occur fully during the initial

stage, and the nanocrystallites with  $d_m = 10\text{--}20\text{ nm}$  are embedded in a residual amorphous matrix<sup>[10]</sup>. So it is reasonable to assume that when the amorphous phase was crystallized into the crystalline state with small grain sizes, the several vacancy-sized free volumes developed into one vacancy-sized defect during crystallization.

However, there are different dependences of positron lifetimes on heating temperature or time due to the structural relaxation or grain growth, as shown in Figs. 3 and 4. The intensity ( $I_1$  and  $I_2$ ) fluctuation symbolizes the changes of the free volumes in the heated amorphous samples. When the amorphous sample was heated at  $200\text{ }^\circ\text{C}$ , the positron lifetimes changed through varied intensity and the decrease of the mean lifetime after structural relaxation, indicating that the average size of the free volume fluctuations decrease slightly during this process. When the heating temperature increased up to  $400\text{ }^\circ\text{C}$ , the amorphous structure was further relaxed in parallel with the increase in mean positron lifetime, indicating that a new type of free volumes was formed with different sizes. The two main lifetime components are confirmed that the vacancy-type free volumes at intergranular layers and the microvoids scaled as several missing atoms space among relaxed atomic aggregates are contributed. Lower temperature annealing induced a change in the free volumes, which is attributed to atomic rearrangement in the amorphous state that continuously lowers the free energy of the system. Nagel et al<sup>[11]</sup> related that the relaxed free volumes in the bulk glasses can be restored by heat treatment above  $T_g$ . So the temperature-dependent redistribution of the positrons among the trapping centers is naturally confirmed, that can be evidenced by the changes in the two components with different intensities. Further heated to higher temperature, the relaxed atomic sites gradually developed to the nuclei of crystallization. With the evolution of the crystallization, the amorphous structure is subjected to the atomic arrangements with larger scale leading to a decrease in the mean lifetime. This second stage that occurs at relatively higher temperature is towards the nanocrystallization process until  $680\text{ }^\circ\text{C}$ . Therefore, the structural relaxation of the amorphous  $\text{Pr}_2\text{Fe}_{14}\text{B}$  results in changes in free volume distributions before nanocrystallization due to the atomic rearrangements.

When the nanocrystalline state developed into crystallites with larger grain sizes, the similarity between the as-prepared amorphous and the initial nanocrystalline specimens was destroyed leading to the two components with different positron lifetimes. Fig. 4 shows the dependence of the positron lifetimes and the relative intensities on annealing time (grain growth) after nanocrystallization, ranging from 5 min to 300 min. Changes in free volumes with differ-

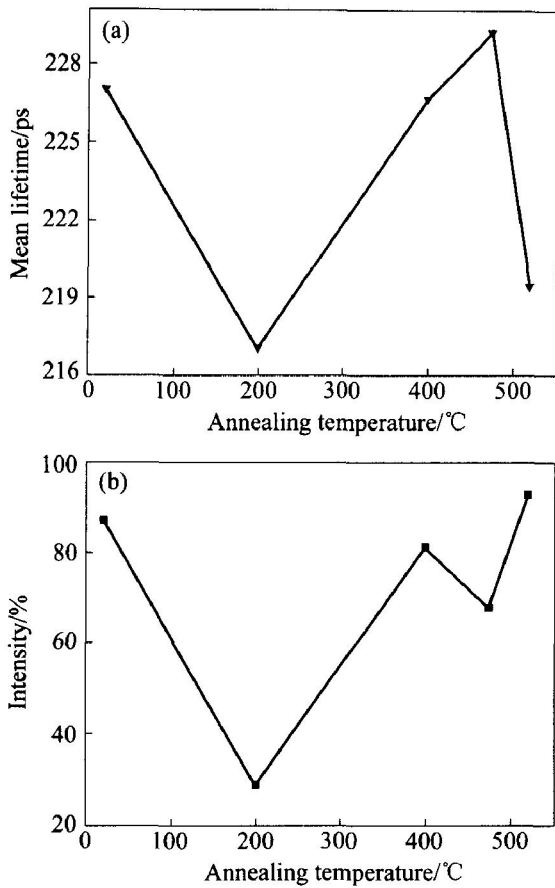


**Fig. 3** Mean lifetime ( $\tau_m$ ) and intensity ( $I_1$ ) of amorphous  $\text{Pr}_2\text{Fe}_{14}\text{B}$  as subjected to heating at relatively lower temperature fluctuated with step heating temperature, indicating that the interfacial free volumes changed with respect to structural relaxation

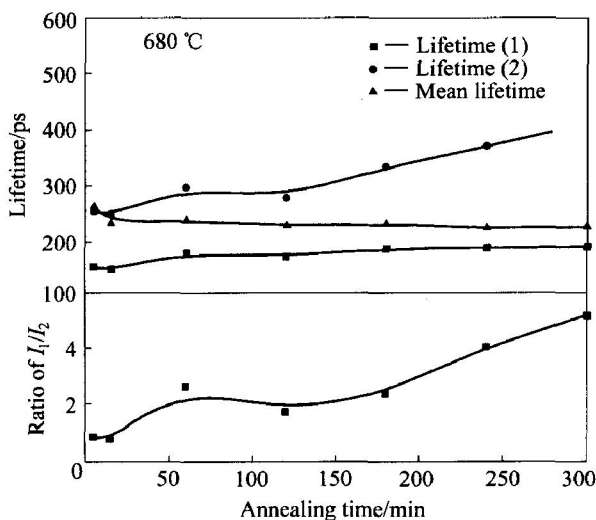


**Fig. 4** Changes of positron lifetime ( $\tau_1$  and  $\tau_2$ ) and intensity ratio of  $I_1/I_2$  of nanocrystalline  $\text{Pr}_2\text{Fe}_{14}\text{B}$  with annealing time at 680 °C after nanocrystallization

the positron lifetime of nanocrystalline iron changed from the defect-free value 106 ps to 175 ps for the monovacancy lifetime. The features of the free volumes existing in the nanocrystalline state according to the data of defect-free crystallite can be determined. The positron annihilation spectra of the nanocrystallized  $\text{Pr}_2\text{Fe}_{14}\text{B}$  mainly consist of two components  $\tau_1$  and  $\tau_2$ , obviously revealing that all the positrons were efficiently trapped into free volumes in the interfaces of the nanocrystalline  $\text{Pr}_2\text{Fe}_{14}\text{B}$ . A wide distribution of interatomic distances in the interfaces is expected due to the great number of different structures of the interfaces<sup>[13]</sup>. The above results show that two kinds of defects (vacancies and microvoids) exist at the interfaces in the nanocrystalline specimens.

However, according to the reversed changes in intensity of  $\tau_1$  and  $\tau_2$ , the contributions from the two components can be explained from two aspects. First, the increase of lifetimes  $\tau_1$  and  $\tau_2$  demonstrates that the free volumes still exist during the grain growth in the annealing process and, the first type defect located at the interfaces will be principally developed. On the other hand, when the annealing time was prolonged to 300 min, the grain sizes of the nanocrystalline  $\text{Pr}_2\text{Fe}_{14}\text{B}$  were still limited to 100 nm. The main free path of a free positron in a defect-free crystal is about 100 nm<sup>[14]</sup>, so a dominant part of the positrons injected into the specimens were annihilated in vacancy-type sites at the interfaces of the nanocrystallites. The densification of the material and a significant decrease of the interface component cause the decrease of the mean positron lifetime by atomic rearrangement. The second type defect will be gradually eliminated with increasing grain size, only vacancy sized free volumes reside in the grain boundaries of the nanocrystallite  $\text{Pr}_2\text{Fe}_{14}\text{B}$ . The interpretation of  $\tau_1$  by vacancy-size traps in the crystallite boundaries is supported by the increase in the intensity ratio of  $I_1/I_2$  with the grain growth.

Therefore, the annealing created nanocrystalline states with different size distributions and structural changes, resulting in different changes between the two kinds of free volumes. The prolonged time annealing was assumed to increase the interfacial areas due to the structural relaxations and grain growth, and thereby the large density of vacancy-size traps. Moreover, it is not difficult to find that at the initial heating stages (shorter annealing time), i. e., small grain size, and the first component with positron lifetime values between  $\tau_1$  and  $\tau_1$  is observed. As related to the positron-trapping mechanism at grain bound-

ent tendencies have appeared during this process. Schaefer et al<sup>[12]</sup> comprehensively demonstrated that

aries, Hidalgo et al.<sup>[15]</sup> indicated that grain boundaries contain shallow traps for positrons. The shorter lifetime corresponded to trapping at regions of low atomic density associated with grain boundaries with an electron density higher than the one associated with a vacancy. Certainly, the effect of the first component is seen mainly on the second component, whose intensity decreased with the grain growth due to the increase of the positron diffusion length.

In the case of saturation trapping, trapping rates  $\sigma_i \tau_i$  are correlated to the intensities by  $I_i = \sigma_i \tau_i / (1/\tau_0 + 1/\tau_i)$ , where  $\tau_i$  denotes specific trapping rates of various types,  $i$ , of traps. When the thermalized positrons are trapped at interfacial vacancies and microvoids,  $\tau_0$  can be neglected due to their long diffusion length  $L_{\text{eff}} = 100$  nm in crystalline bulk metals<sup>[12]</sup>. Assuming equal trapping rates per unit area of interfaces for the two kinds of defect, the interface-area ratio of the two kinds of defect may be estimated by using the experimental results of  $I_1/I_2$  based on the relation:  $\sigma_1 \tau_1 / \sigma_2 \tau_2 = I_1/I_2$ . The increase of  $I_1/I_2$  with increasing grain size means that, in a unit area of interfaces, there are more monovacancy-type interfacial defects and fewer microvoid-type defects during grain growth. However, the concentrations of the defects in the interfaces can not be determined directly from the experimental data. In the nanocrystalline iron, it has been reported that the ration of interfaces with monovacancy defects between the crystallites to the crystallites-microvoid interfaces is in the range of 0.5 - 1.0<sup>[12]</sup>. In our studied materials, the surface ratio of interfaces in comparison with the main two defects is up to 9.4. The research topic about the interfacial structures and defects transformation<sup>[16]</sup> will be further discussed.

#### 4 SUMMARY

In conclusion, similar changes in the positron lifetimes between the amorphous precursor and the initial nanocrystalline states of Pr<sub>2</sub>Fe<sub>14</sub>B were found. The first lifetime ( $\tau_1$ ) is attributed to vacancy-type defects in the intergranular layers or the interfacial regions between the crystallites with dominant intensity, and the second one ( $\tau_2$ ) is assigned to the intersections among the aggregated atoms or the microvoids in the interfaces. For the amorphous specimen subjected to annealing at relatively lower temperature, the positron lifetime underwent different changes between the two components due to the structural fluctuations during the structural relax-

ation. For the nanocrystalline Pr<sub>2</sub>Fe<sub>14</sub>B, as the anneal time was prolonged (grain size increased), although the two lifetimes increased to different extents, the mean lifetime ( $\tau_m$ ) for the nanocrystal decreases and the intensity ratio of  $I_1/I_2$  increases with increasing grain size. The two type defects will be transformed with increasing grain size.

#### ACKNOWLEDGEMENTS

The author (Y. C. Wu) would like to thank Professor H. E. Schaefer and Dr. W. Sprengel, K. Reimann, K. J. Reichle (Institut für Theoretische und Angewandte Physik, Universität Stuttgart, Germany) and Professor R. Würschum (Institut für Technische Physik, Universität Graz, Austria) for their help during his visiting research in Institut für Theoretische und Angewandte Physik, Universität Stuttgart, Germany. He also thanks Dr. D. Goll of Max-Planck-Institut für Metallforschung for her providing specimen materials.

#### REFERENCES

- [1] Kronmüller D G. High performance permanent magnets [J]. *Naturwissenschaften*, 2000, 87: 423.
- [2] Kronmüller H, Fischer R, Bachmann M, et al. Magnetization processes in small particles and nanocrystalline [J]. *J Mag Mag Mater*, 1999, 203: 12 - 17.
- [3] Kojima A, Makino A, Inoue A. Rapid annealing effect on the microstructure and magnetic properties of the Fe-rich nanocomposite magnets [J]. *J Appl Phys*, 2000, 87: 6576 - 6578.
- [4] Fidler J, Schrefl T. Overview of Nd-Fe-B magnets and coercivity (invited) [J]. *J Appl Phys*, 1996, 79: 5029.
- [5] Seeger A. Challenges to positron and positronium physics by materials science [J]. *Mater Sci Forum*, 1997, 1: 255 - 257.
- [6] Schaefer H-E, Banhart F. Thermal equilibrium vacancies in platinum studied by positron annihilation [J]. *Phys Stat Sol (a)*, 1987, 263: 104.
- [7] Dittmar R, Würschum R, Ulfer W, et al. Crystallization and thermal vacancy formation in Fe<sub>73.5</sub>Si<sub>13.5</sub>B<sub>9</sub>Nb<sub>3</sub>Cu<sub>1</sub> and Zr<sub>65</sub>Cu<sub>17.5</sub>Ni<sub>10</sub>Al<sub>7.5</sub> [J]. *Mater Sci Forum*, 1997, 255 - 257: 530.
- [8] Baier F, Müller M A, Grushko B, et al. Atomic defects in quasicrystals: an approach with positron annihilation spectroscopy and time differential dilatometry [J]. *Mater Sci Eng*, 2000, 294 - 296: 650.
- [9] Nagel C, Rätzke K, Schmidtke E, et al. Free volume changes in the bulk metallic glass Zr<sub>46.7</sub>Ti<sub>8.3</sub>Cu<sub>7.5</sub>Ni<sub>10</sub>Be<sub>27.5</sub> and the undercooled liquid [J]. *Phys Rev B*, 1998, 57: 10224.
- [10] Balogh J, Bujdosó L, Kaptas D, et al. Hyperfine field at grain boundary atoms in iron nanostructures [J]. *Hy-*



- perfine Interactions, 2000, 126: 171.
- [ 11] Nagel C, Rätzke K, Schmidtke E, et al. Positron annihilation of free volume changes in the bulk metallic glass  $\text{Zr}_{65}\text{Al}_{7.5}\text{Ni}_{10}\text{Cu}_{17.5}$  during structural relaxation and at the glass transition [ J]. Phys Rev B, 1999, 60: 9212.
- [ 12] Schaefer H-E, Würschum R, Birringer R, et al. Structure of nanometer-sized polycrystalline iron investigated by positron lifetime spectroscopy [ J]. Phys Rev B, 1998, 38: 9545.
- [ 13] Balogh J, Bujdosó L, Kaptas D, et al. Mössbauer study of the interface of iron nanocrystallites [ J]. Phys Rev B, 2000, 61: 4109.
- [ 14] Pasquini L, Rempel A A, Würschum R, et al. Thermal vacancy formation and  $\text{DO}_3$  ordering in nanocrystalline intermetallic  $(\text{Fe}_3\text{Si})_{95}\text{Nb}_5$  [ J]. Phys Rev B, 2001, 63: 134114.
- [ 15] Hidalgo C. de Diego N, Plazaola F. Positron trapping mechanism at grain boundaries [ J]. Phys Rev B, 1985, 31: 6941.
- [ 16] Wu Y C, Sprengel W, Reimann K, et al. Structural Evolution of Nanocrystalline  $\text{Pr}_2\text{Fe}_{14}\text{B}$  Studied by Positron Spectroscopy Techniques [ R]. DPG, Regensburg, Germany, 2002.

( Edited by PENG Chao-qun)